the FeH_3P_3 unit, and this octahedral unit then remains stereochemically rigid in the product. The $(H)_3Cu$ ligation of copper in the product represents an unusually high hydride-to-copper ratio among known copper hydrides. Note, for comparison, that the reaction of $Cu(NCMe)_4^+$ with *mer*-$IrH_3(PMe_2Ph)_3$ gives $Cu[H_3Ir(PMe_2Ph)_3]_2^+$ where the *mer* stereochemistry is retained at iridium.[35]

(2) In the reaction with $WH_2(CO)_3(PR_3)_2$ (**2**), only one hydride is available to bridge to copper. Moreover, there is infrared evidence supporting the possibility of a bridging carbonyl ligand, providing a higher coordination number for copper.

(3) In all of the above reactions, if $[Cu(O\text{-}t\text{-}Bu)]_4$ is employed rather than $[Cu(O\text{-}t\text{-}Bu)(PR_3)]_2$, the coordination requirements of Cu^+ are supplemented by one phosphine scavenged from the phosphine/dihydrogen reaction partner. This phosphine scavenging is possible because the dihydrogen reagents are generally fragile molecules, and their concurrent decomposition can release PR_3. The absence of aggregated products of the sort $L_nM_3Cu_3$ (analogous to I) is due at least in part to this availability of phosphine.

The reactions described here are all fast (i.e., time-of-mixing). They are thus unlike substitution reactions on kinetically inert low-spin d^6 species. This suggests either Lewis acid/base or proton transfer mechanisms.

Acknowledgment. This work was supported by the National Science Foundation (at Indiana University) and the Office of Energy Research, Division of Chemical Sciences, U.S. Department of Energy. We also thank Timothy H. Lemmen and William G. Van Der Sluys for helpful discussion and Stephen W. Hall for skilled technical assistance.

Registry No. 1, 102149-40-6; **2a**, 104198-75-6; **2b**, 125875-90-3; **2c**, 125593-90-0; **2d**, 104198-78-9; **3**, 132233-13-7; **4a**, 132233-14-8; **4b**, 132233-17-1; **4c**, 132233-18-2; IV, 132233-22-8; $W(CO)_3(PCy_3)_2$, 73690-56-9; $[CuH(PPh_3)]_6$, 33636-93-0; $[Cu(O\text{-}t\text{-}Bu)(PPh_3)]_2$, 106761-46-0; $[CuO\text{-}t\text{-}Bu]_4$, 60842-00-4; $[Cu(O\text{-}t\text{-}Bu)(PCy_3)]_2$, 132233-15-9; $[Cu(O\text{-}t\text{-}Bu)(PPhzEt)]_2$, 132233-16-0; $(PCy_3)(PPh_2Et)(CO)_3W(\mu\text{-}H)Cu(PPh_2Et)$, 132233-19-3; $(PCy_3)(CO)_3W(\mu\text{-}H)Cu(PPh_2Et)$, 132233-20-6; $[Cu(O_2CH)(PEtPh_2)]$, 132233-21-7; $[W(CO)_3(PCy_3)_2(O\text{-}t\text{-}Bu)Cu]$, 132233-23-9.

Supplementary Material Available: Tables of anisotropic displacement coefficients for $(PEtPh_2)_3Fe(\mu\text{-}H)_3Cu(PEtPh_2)$, H-atom coordinates ($\times 10^4$) and isotropic displacement coefficients, and atomic coordinates and equivalent isotropic displacement coefficients (6 pages); listing of observed and calculated structure factor amplitudes for $(PEtPh_2)_3Fe(\mu\text{-}H)_3Cu(PEtPh_2)$ (13 pages). Ordering information is given on any current masthead page.

(35) Rhodes, L. F.; Huffman, J. C.; Caulton, K. G. *J. Am. Chem. Soc.* **1984**, *106*, 6874.

Cone Angles for Amine Ligands. X-ray Crystal Structures and Equilibrium Measurements for Ammonia, Ethylamine, Diethylamine, and Triethylamine Complexes with the (Bis(dimethylphosphino)ethane)methylpalladium(II) Cation

Allen L. Seligson and William C. Trogler*

Contribution from the Department of Chemistry, University of California, San Diego, La Jolla, California 92093-0506. *Received September 12, 1990*

Abstract: The reaction between $Pd(dmpe)Me_2$, where dmpe = 1,2-bis(dimethylphosphino)ethane, and $[NH_4]PF_6$, $[NH_4]BPh_4$, $[NH_3Et]BPh_4$, $[NH_2Et_2]BF_4$, $[NH_2Et_2]BPh_4$, $[NHEt_3]BPh_4$, $[NH_2^iPr_2]BPh_4$, and [1-methylimidazolium]BPh_4 in CH_2Cl_2 or CH_3CN solvent rapidly produces CH_4 and the corresponding amine complexes $[Pd(dmpe)CH_3(NRR'R'')]X$, **1-8**, respectively. All can be isolated as crystalline solids in 57-87% yield. Crystals of **1** belong to the monoclinic space group $P2_1/c$ with lattice constants a = 8.378 (5) Å, b = 16.696 (8) Å, c = 12.024 (5) Å, β = 103.91 (4)°, and Z = 4. **3** crystallizes in the monoclinic space group $P2_1/c$ with lattice constants a = 9.986 (3) Å, b = 11.024 (4) Å, c = 29.601 (9) Å, β = 92.69 (2)°, and Z = 4. **4** crystallizes in the orthorhombic space group *Pbcn* with lattice constants a = 13.181 (4) Å, b = 23.897 (7) Å, c = 24.854 (9) Å, and Z = 16. **6** crystallizes in the monoclinic space group $P2_1/c$ with lattice constants a = 9.566 (4) Å, b = 21.773 (7) Å, c = 17.662 (5) Å, β = 90.62 (3)°, and Z = 4. Least-squares refinement of the structures led to R factors of 0.047, 0.054, 0.055, and 0.054, respectively. All complexes adopt a square-planar geometry with angle distortions in the plane, which parallel the increasing size of the amine. The Pd-N bond lengths of 2.139 (5), 2.174 (6), 2.182 (8), and 2.244 (7) Å in **1**, **3**, **4**, and **6** correlate linearly with the steric cone angle for the amine ligands. The Pd-N bond length in **6** exceeds that of 2.201 (3) Å for the trans Pd-P bond, which reflects severe steric crowding for the triethylamine ligand. Cone angles for these and other amines were determined from geometric measurements of CPK models. Equilibrium binding constants for 16 amine ligands to the $Pd(dmpe)Me^+$ Lewis acid were measured by variable-temperature ^{31}P NMR spectroscopy. Binding constants for amines of similar pK_a correlate well with the amine cone angles, θ; however, a steric threshold was observed when $\theta \leq 120°$. Binding constants, relative to the $NHEt_2$ complex, K, for the ligands obeyed the relationship $\log K = 8.1 + 0.54pK_a - 0.15\theta$, with a correlation coefficient of 0.95. This shows a dependence on both electronic and steric properties of the amine ligands. Of the various amine ligands studied, 1-methylimidazole and ethylamine bind most effectively. This parallels the role of histidine and lysine for binding metals in metalloproteins.

Introduction

The cone angle concept, developed by Tolman,[1] has been widely accepted by organometallic chemists as a quantitative measure of steric effects for trivalent phosphorus ligands.[2] Cone angles have been used not only to explain structural and thermodynamic aspects of metal complexes[3] but also to construct linear free energy

(1) Tolman C. A. *J. Am. Chem. Soc.* **1970**, *92*, 2956-2965.

(2) Collman, J. P.; Hegedus, L. S.; Norton, J. R.; Finke, R. G. *Principles and Applications of Organotransition Metal Chemistry*; University Science Books: Mill Valley, CA, 1987; Chapter 3.

(3) Tolman, C. A. *Chem. Rev.* **1988**, *77*, 313-348.

0002-7863/91/1513-2520$02.50/0

relationships in numerous reactivity correlations.[4] Even NMR chemical shift data has been shown to correlate with phosphorus ligand size.[5] In assessing the electronic basicity of phosphine ligands either the A_1 carbonyl stretching frequency for a series of $Ni(CO)_3(PR_3)$ complexes or the pK_a of the PR_3 ligand has been used with success.[4]

Amines are ubiquitous ligands in transition-metal chemistry. They bind to metals in enzymes, classical coordination complexes, and organometallic compounds. In spite of their importance we could find no quantitative information about the steric properties of amines to guide us in our ongoing studies of olefin insertion reactions into metal–nitrogen bonds.[6] Amine ligand reactivity correlations for metal complexes have primarily focused on pK_a trends.[4,7,8] Steric effects were qualitatively considered in studies of the binding of substituted pyridines to copper carboxylates[9] and of the thermodynamics of amine binding to the $Cr(CO)_5$ fragment.[10]

Previous to all this work Brown[11] showed the importance of steric effects on the formation of Lewis acid–base complexes between amines and alkyl boranes. He introduced the now classic concepts of F- and B-strain, which seemed to account for anomalies in pK_a-binding constant correlations. In these studies the amine pK_a was employed as an electronic parameter, and the steric contribution of these ligands was considered qualitatively.

We have chosen the $Pd(dmpe)Me^+$ fragment, which forms a wide range of amine complexes, to measure relative equilibrium binding constants for a range of sterically and electronically varied amines. Here we attempt to separate these two parameters and use cone angles to place amine and phosphine ligands on a common steric scale. Crystal structure analyses for a series of amine complexes have been determined to provide information about the structural consequences of varying ligand size.

Experimental Section

All reactions were performed under a nitrogen atmosphere by using modified Schlenk techniques. Liquids were transferred by syringe (or cannula). Materials obtained from commercial sources were used without purification except where noted. Under a nitrogen atmosphere, CH_3CN and CH_2Cl_2 were distilled from CaH_2, and Et_2O was distilled from sodium benzophenone ketyl. The complex $Pd(dmpe)Me_2$ was prepared by a literature procedure.[12] Ammonium salts of the type $[HNRR'R''][BPh_4]$ were prepared from the reaction between $NaBPh_4$ and the corresponding hydrochloride salt in H_2O. For equilibrium measurements, all amine solutions were prepared under a nitrogen purge. Elemental analyses were performed by Oneida Research Services. IR spectra were recorded with the use of an IBM IR/32 FTIR spectrometer. All NMR spectra were recorded on a GE QE-300 MHz NMR equipped with a 5-mm broad band probe. ^1H NMR spectra chemical shifts were referenced to the residue solvent peaks in observed spectra. The ^{31}P NMR spectra were referenced to the deuterated lock solvent, which had been previously referenced to 85% H_3PO_4. All ^{31}P shifts were recorded relative to H_3PO_4 with downfield shifts being positive.

Ammine(bis(dimethylphosphino)ethane)methylpalladium(II) Tetraphenylborate, [Pd(dmpe)Me(NH$_3$)][BPh$_4$], 2. To a solution of Pd(dmpe)Me_2 (0.206 g, 0.71 mmol) in degassed CH_3CN (10 mL) was added a solution of $[NH_4][BPh_4]$ (0.240 g, 0.71 mmol) in 5 mL of ammonia-saturated CH_3CN (bubbling NH_3 gas through a suspension of $[NH_4][BPh_4]$ in CH_3CN causes the salt to dissolve). Evolution of gas occurs immediately after addition, and the solution was stirred 15 min. The solution was filtered, concentrated to ~5 mL, purged with NH_3 gas for several minutes, and they layered with Et_2O (~15 mL) to yield colorless crystals of **2**, 0.381 g (87%): mp dec 108–120 °C; ^1H NMR (CD_2Cl_2) –0.005 (dd, $^3J_{P-H(trans)}$ = 7.2 Hz, $^3J_{PH(cis)}$ = 2.9 Hz, 3 H, PdCH_3), 0.578 (s br, 3 H, PdNH_3), 1.23 (d, $^2J_{PH}$ = 8.2 Hz, 6 H, PCH_3), 1.44 (d, $^2J_{P-H}$ = 10.9 Hz, 6 H, PCH_3), 1.52 and 1.74 (m, 4 H, PCH_2), 6.90 (tr, 4 H, BPh_4), 7.06 (tr, 8 H, BPh_4), 7.44 (m br, 8 H, BPh_4); IR (KBr, cm^{-1}) 3346, 3273 (N–H). Anal. Calcd for $C_{31}H_{42}BNP_2Pd$: C, 61.25; H, 6.96; N, 2.30. Found: C, 62.03; H, 7.28; N, 2.40.

Ammine(bis(dimethylphosphino)ethane)methylpalladium(II) Hexafluorophosphate, [Pd(dmpe)Me(NH$_3$)][PF$_6$], 1. This complex was prepared by a similar procedure as above with $[NH_4][PF_6]$: yield 82%; mp dec 110–150 °C; ^1H NMR (CD_2Cl_2) 0.224 (dd, $^3J_{PH(trans)}$ = 7.1 Hz, $^3J_{PH(cis)}$ = 2.8 Hz, 3 H, PdCH_3), 2.36 (s br, 3 H, PdNH_3), 1.40 (d, $^2J_{PH}$ = 8.4 Hz, 6 H, PCH_3), 1.56 (d, $^2J_{PH}$ = 11.3 Hz, 6 H, PCH_3), 1.73 and 1.94 (m, 4 H, PCH_2); IR (KBr, cm^{-1}) 3360, 3397 (N–H). Anal. Calcd for $C_7H_{22}F_6NP_3Pd$: C, 19.39; H, 5.11; N, 3.23. Found: C, 19.34; H, 4.91; N, 3.15.

(Bis(dimethylphosphino)ethane)(ethylamine)methylpalladium(II) Tetraphenylborate, [Pd(dmpe)Me(NH$_2$Et)][BPh$_4$], 3. To a solution of Pd(dmpe)Me_2 (0.264 g, 0.92 mmol) in CH_3CN (10 mL) and NH_2Et (2 mL) was added solid $[NH_3Et][BPh_4]$ (0.337 g, 0.02 mmol). Evolution of gas was observed, and the colorless reaction solution was allowed to stir for 15 min. The solution was filtered, and the colorless filtrate was concentrated to 2–4 mL. After addition of 1 mL of NH_2Et the solution was layered with Et_2O (~10 mL) to yield colorless crystals of **3**, 0.399 g (68%): mp dec 130–150 °C; ^1H NMR (CD_2Cl_2) 0.146 (dd, $^3J_{PH(trans)}$ = 6.8 Hz, $^3J_{PH(cis)}$ = 2.9 Hz, 3 H, PdCH_3), 1.05 (t, 3 H, CH_2CH_3), 2.55 (q, 2 H, NH_2CH_2), 1.94 (s br, 2 H NH_2), 1.28 (d, $^2J_{PH}$ = 8.0 Hz, 6 H, PCH_3), 1.47 (d, $^2J_{PH}$ = 10.9 Hz, 6 H, PCH_3), 1.55 and 1.75 (m, 4 H, PCH_2), 6.91 (t, 4 H, BPh), 7.06 (t, 8 H, BPh), 7.36 (m br, 8 H, BPh); IR (KBr, cm^{-1}) 3316, 3272 (N–H). Anal. Calcd for $C_{33}H_{46}BNP_2Pd$: C, 62.33; H, 7.29; N, 2.20. Found: C, 62.02; H, 7.42; N, 2.21.

(Diethylamine)(bis(dimethylphosphino)ethane)methylpalladium(II) Tetraphenylborate, [Pd(dmpe)Me(NHEt$_2$)][BPh$_4$], 5. To a solution of Pd(dmpe)Me_2 (0.303 g, 1.06 mmol) in CH_3CN (15 mL) and $NHEt_2$ (1 mL) was added solid $[NH_2Et_2][BPh_4]$ (0.416 g, 1.06 mmol). On addition immediate evolution of gas was observed to yield a colorless solution, and stirring was continued for 15 min. The solution was filtered, and the resultant filtrate was concentrated to 2–4 mL. After addition of 1 mL of $NHEt_2$ the solution was layered with Et_2O (~15 mL) to produce colorless crystals of **5**, 0.519 g (73%): mp dec 120–140 °C; ^1H NMR (CD_2Cl_2) 0.245 (dd, $^3J_{PH(trans)}$ = 6.7 Hz, $^3J_{PH(cis)}$ = 2.8 Hz, 3 H, PdCH_3), 1.27 (t, 6 H, CH_2CH_3), 2.66 (m, 2 H, NHCH_2), 2.95 (m, 2 H, NHCH_2), 2.66 (s br, 1 H, NH), 1.34 (d, $^2J_{PH}$ = 7.6 Hz, 6 H, PCH_3), 1.46 (d, $^2J_{PH}$ = 10.9 Hz, 6 H, PCH_3), 1.55 and 1.73 (m, 4 H, PCH_2), 6.91 (tr, 4 H, BPh_4), 7.06 (tr, 8 H, BPh_4), 7.35 (m br, 8 H, BPh_4); IR (KBr, cm^{-1}) 3245 (N–H). Anal. Calcd for $C_{35}H_{50}BNP_2Pd$: C, 63.31; H, 7.59; N, 2.11. Found: C, 63.39; H, 7.35; N, 2.16.

(Diethylamine)(bis(dimethylphosphino)ethane)methylpalladium(II) Tetrafluoroborate, [Pd(dmpe)(Me)(NHEt$_2$)][BF$_4$], 4. This complex was synthesized by a procedure similar to **5** by using $[NH_2Et_2][BF_4]$ to give a 76% yield: mp dec 115–138 °C; ^1H NMR (CD_2Cl_2) 0.229 (dd, $^3J_{PH(trans)}$ = 6.6 Hz, $^3J_{PH(cis)}$ = 2.7 Hz, 3 H, PdCH_3), 1.28 (t, 6 H, CH_2CH_3), 2.71 (m, 2 H, NHCH_2), 2.96 (m, 2 H, NHCH_2), 3.64 (s br, 1 H, NH), 1.51 (d, $^2J_{PH}$ = 8.2 Hz, 6 H, PCH_3), 1.55 (d, $^2J_{PH}$ = 10.9 Hz, 6 H, PCH_3), 1.78 and 1.93 (m, 4 H, PCH_2); IR (KBr, cm^{-1}) 3264, 3384 (N–H). Anal. Calcd for $C_{11}H_{30}BF_4NP_2Pd$: C, 30.62; H, 7.01; N, 3.25. Found: C, 30.76; H, 6.97; N, 3.27.

(Bis(dimethylphosphino)ethane)(triethylamine)methylpalladium(II) Tetraphenylborate, [Pd(dmpe)(Me)(NEt$_3$)][BPh$_4$], 6. To a solution of Pd(dmpe)Me_2 (0.253 g, 0.88 mmol) in CH_3CN (10 mL) and NEt_3 (3 mL) was added solid $[NEt_3H][BPh_4]$ (0.37 g, 0.88 mmol). On addition there was immediate evolution of gas, and the colorless solution was allowed to stir for 15 min. The solution was filtered, and the filtrate was concentrated to 2–4 mL. To this was added NEt_3 (0.5 mL), and the solution was layered with Et_2O (~15 mL) and cooled to –40 °C to obtain olive-colored crystals of **6**, 0.347 g (57%). This complex is thermally sensitive and decomposes in solution unless excess NEt_3 is present: mp dec 98–110 °C; ^1H NMR (CD_2Cl_2) 0.28 (dd, $^3J_{PH(trans)}$ = 5.8 Hz, 3 H, PCH_3), 1.18 (t, 9 H, CH_2CH_3), 2.82 (q, 6 H, NCH_2), 1.34 (d, $^2J_{PH}$ =

(4) (a) Liu, H.-Y.; Eriks, K.; Prock, A.; Giering, W. P. *Organometallics* **1990**, *9*, 1758–1766. (b) Eriks, K.; Giering, W. P.; Liu, Y.-Y.; Prock, A. *Inorg. Chem.* **1989**, *28*, 1759–1763. (c) Rahman, M. M.; Liu, H.-Y.; Eriks, K.; Prock, A.; Giering, W. P. *Organometallics* **1989**, *8*, 1-7. (d) Rahman, M. M.; Liu, H.-Y.; Prock, A.; Giering, W. P. *Organometallics* **1987**, *61*, 650–658. (e) Golovin, M. N.; Rahman, M. M.; Belmonte, J. E.; Giering, W. P. *Organometallics* **1985**, *4*, 1981–1991. (f) Lee, K.-W.; Brown, T. L. *Inorg. Chem.* **1987**, *26*, 1852–1856. (g) Gao, Y.-C.; Shi, Q.-Z.; Kershner, D. L.; Basolo, F. *Inorg. Chem.* **1988**, *27*, 188–191. (h) Dahlinger, K.; Falcone, F.; Poë, A. J. *Inorg. Chem.* **1986**, *25*, 2654–2658. (i) Zizelman, P. M.; Amatore, C.; Kochi, J. K. *J. Am. Chem. Soc.* **1984**, *106*, 3771–3784. (j) Baker, R. T.; Calabrese, J. C.; Krusic, P. J.; Therien, M. J.; Trogler, W. C. *J. Am. Chem. Soc.* **1988**, *110*, 8392–8412.

(5) Trogler, W. C.; Marzilli, L. G. *J. Am. Chem. Soc.* **1974**, *96*, 7589. (b) Clark, H. C.; Nicholas, A. M. *Magn. Reson. Chem.* **1990**, *28*, 99–103.

(6) (a) Cowan, R. L.; Trogler, W. C. *J. Am. Chem. Soc.* **1989**, *111*, 4750–4761. (b) Seligson, A. L.; Trogler, W. C., results to be published.

(7) Dennenberg, R. J.; Darensbourg, D. J. *Inorg. Chem.* **1972**, *11*, 72–77.

(8) Therien, M. J.; Trogler, W. C. *J. Am. Chem. Soc.* **1987**, *109*, 5127–5133.

(9) Uruska, I.; Zielkiewicz, J.; Szpakowska, M. *J. Am. Chem. Soc., Dalton Trans.* **1990**, 733–736.

(10) Burkey, T. J. *Polyhedron* **1989**, *8*, 2681–2687.

(11) Brown, H. C. *Boranes in Organic Chemistry*; Cornell University Press: Ithaca, NY, 1972.

(12) Tooze, R.; Chiu, K. W.; Wilkinson, G. *Polyhedron* **1984**, *3*, 1025–1028.

Table I. Crystallographic Data and Summary of Data Collection and Refinement for [Pd(dmpe)Me(NRR'R'')]X Complexes

	1	3	4	6
formula	$C_7H_{22}NR_6P_3Pd$	$C_{33}H_{46}NBP_2Pd$	$C_{11}H_{30}BNF_4P_2Pd$	$C_{37}H_{54}BNP_2Pd$
fw	433.59	635.92	432.54	692.03
crystal system	monoclinic	monoclinic	orthorhombic	monoclinic
space group	$P2_1/c$	$P2_1/c$	$Pbcn$	$P2_1/c$
a, Å	8.378 (5)	9.986 (3)	13.181 (4)	9.566 (4)
b, Å	16.696 (8)	11.024 (4)	23.897 (7)	21.773 (7)
c, Å	12.024 (5)	29.601 (9)	24.854 (9)	17.662 (5)
β, deg	103.91 (4)	92.69 (2)		90.62 (3)
V, Å^3	1632.5 (15)	3255.1 (14)	7828 (4)	3678 (2)
d_{calc}, g cm^{-3}	1.764	1.297	1.464	1.250
μ, mm^{-1}	1.454	0.679	1.121	0.606
scan type	ω-2θ	ω	ω	ω
no. unique data	4777	6750	6882	4806
no. reflcns used $I > 3\sigma(I)$	3930	3914	4173	2909
no. parameters	148	164	326	244
Z	4	4	16	4
scan range (°)	$4.0 < 2\theta < 60.0°$	$3.0 < 2\theta < 53.0$	$4.0 < 2 < 50.0$	$3.0 < 2 < 45.0$
largest residual peak, e/Å^3	1.01	0.88	0.99	0.81
R	0.047	0.054	0.055	0.054
R_w	0.093	0.067	0.096	0.061
GOF	0.63	1.62	0.35	1.74

7.2 Hz, 6 H, PCH_3), 1.46 (d, $^2J_{PH}$ = 10.9 Hz, 6 H, PCH_3), 1.66 (m, 4 H, PCH_2), 6.90 (t, 4 H, BPh_4), 7.05 (t, 8 H, BPh_4), 7.34 (s br, 8 H, BPh). Anal. Calcd for $C_{37}H_{54}BNP_2Pd$: C, 64.22; H, 7.86; N, 2.02. Found: C, 64.07; H, 7.80; N, 2.11.

(Bis(dimethylphosphino)ethane)(diisopropylamine)methylpalladium(II) Tetraphenylborate, [Pd(dmpe)Me(NH^{i}Pr$_2$)][BPh$_4$], 7. To a solution of Pd(dmpe)Me_2 (0.265 g, 0.92 mmol) in CH_2Cl_2 (3 mL) and NH^{i}Pr$_2$ (2 mL) was added solid [NH$_2^i$Pr$_2$][BPh_4] (0.390 g, 0.92 mmol). Immediate evolution of gas occurred, and the colorless solution was allowed to stir for 15 min. The solution was filtered, and the filtrate was concentrated to 2–4 mL, layered with NH^{i}Pr$_2$ (~15 mL), and cooled to −40 °C to obtain colorless crystals of **7**, 0.372 g (58%): mp dec 115–122 °C; ^{1}H NMR (CD_2Cl_2) 0.322 (dd, $^3J_{PH(trans)}$ = 5.0 Hz, $^3J_{PH(cis)}$ = 1.5 Hz, 3 H, PdCH_3), 1.22 (d, 12 H, CH(CH_3)$_2$), 3.14 (sep, 2 H NHCH), 2.67 (s br, 1 H, NH), 1.38 (d, $^2J_{PH}$ = 7.6 Hz, 6 H, PCH_3), 1.47 (d, $^2J_{PH}$ = 12.5 Hz, 6 H, PCH_3), 1.6 (m, 4 H, PCH_2), 6.89 (tr, 4 H, BPh_4), 7.04 (tr, 8 H, BPh_4), 7.33 (m br, 8 H, BPh_4); IR (KBr, cm^{-1}) 3245 (NH). Anal. Calcd for $C_{37}H_{54}BNP_2Pd$: C, 64.22; H, 7.86; N, 2.02. Found: C, 64.18; H, 7.40; N, 2.07.

Bis(dimethylphosphino)ethane(1-methylimidazole)methylpalladium(II) Tetraphenylborate, [Pd(dmpe)Me(1-Me-imidazole)][BPh$_4$], 8. To a solution of Pd(dmpe)Me_2 (0.220 g, 0.77 mmol) in CH_3CN (5 mL) was added solid 1-methylimidazolium tetraphenylborate (0.309 g, 0.77 mmol). On addition there was immediate evolution of gas, and the colorless solution was allowed to stir for 15 min. The solution was filtered, and the colorless filtrate was concentrated to 1.5 mL. The solution was then layered with Et_2O (25 mL) to yield colorless crystals of **9**, 0.342 g (66%): mp dec 144–150 °C; ^{1}H NMR (CD_2Cl_2) 0.30 (dd, $^3J_{PH(trans)}$ = 7.4 Hz, $^3J_{PH(cis)}$ = 2.9 Hz, 3 H, PdCH_3), 3.57 (s, 3 H, NCH_3), 1.27 (d, $^2J_{PH}$ = 8.2 Hz, 6 H, PCH_3), 1.53 (d, $^2J_{PH}$ = 10.8 Hz, 6 H, PCH_3), 1.61 and 1.83 (m, 4 H, PCH_2), 6.92 (t, 4 H, BPh), 7.05 (t, 8 H, BPh_4), 7.34 (m br, 8 H, BPh_4); IR (KBr cm^{-1}). Anal. Calcd for $C_{35}H_{45}BN_2P_2Pd$: C, 62.46; H, 6.74; N, 4.18. Found: C, 62.78; H, 6.41; N, 4.27.

Equilibrium Measurements. Solid [Pd(dmpe)Me(NHEt$_2$)][BPh_4] was weighed into a NMR tube under a N_2 atmosphere. To this was added CD_2Cl_2 and a predetermined volume of NRR'R''/CH_2Cl_2 solution with stirring until all solid dissolved. The ^{31}P{^{1}H} NMR resonances of the dmpe ligand were recorded at temperatures between −80 °C and 30 °C (because of line broadening at room tempeature). The solutions were equilibrated for 10 min at each temperature. Temperatures were calibrated to the known values for MeOH peak separation. The equilibrium abundance of the two palladium amine species were determined by integration of the phosphorus resonance trans to the nitrogen of the amine. The percent abundance of the two complexes along with the known initial concentrations of the solution allowed for the calculation of the relative equilibrium constant at each temperature. By using van't Hoff plots, equilibrium data at 20 °C could be calculated by extrapolation. The reported values are the averages of three experimental runs. Several values were recorded only at 20 °C, because line broadening from amine exchange was not a problem. Equilibrium values for NH_3, NH_2Et, and 1-methylimidazole were measured by $NHEt_2$ displacement of the coordinated amines from **2**, **3**, and **8**, respectively. Because of solubility limits, the values for NEt_3, quinuclidine, and trimethylamine were calculated stepwise from the equilibrium constants measured from their displacement of **7** and the previously determined value for NH^{i}Pr$_2$ displacement of **5**. Quinuclidine and trimethylamine reacted with CH_2Cl_2 on the time scale of these experiments. Therefore, their equilibrium constants were measured in 80% THF/20% C_6D_6 solvent. We also determined the equilibrium constant for $NH_2{}^tBu$ in this solvent mixture, and its value was nearly the same (0.11 vs 0.13) as that determined in CD_2Cl_2. Equilibrium constants were reproducible to ±10%.

X-ray Structure Determinations. X-ray crystallographic analyses were performed with the use of a Nicolet R3m/V automated diffractometer equipped with a graphite crystal monochrometer and a Mo X-ray tube. Orientation matrix and unit cell parameters were determined by the least-squares fitting of 20 machine-centered reflections ($15° < 2\theta < 30°$) and confirmed by examination of axial photographs. Intensities of three check reflections were monitored every 197 reflections, throughout the data collection. Structure solutions and data workup were performed on a DEC Microvax II computer with SHELXTL PLUS version 3.4 software. Details on crystal and intensity data collection are given in Table I.

A colorless block-shaped crystal of **1** cut to the approximate dimensions 0.62 × 0.53 × 0.43 mm was used for the room-temperature crystal and intensity data collection. The unit cell parameters and systematic absences, $0k0$ ($k = 2 + 1$) and $00l$ ($l = 2n + 1$), unambiguously indicated $P2_1/c$ as the space group. The structure was solved by direct methods. An absorption correction applied from ψ scan data did not significantly improve R, and therefore none was used. All non-hydrogen atoms were refined anisotropically, and the PF_6 anion refined as a rigid group with fixed bond lengths and angles. All hydrogen atoms were generated in idealized positions for the structure factor calculations but were not refined.

A colorless cube-shaped crystal of **3** cut to the approximate dimensions of 0.28 × 0.26 × 0.26 mm was used for the room-temperature crystal and intensity data collection. The unit cell parameters and systematic absences, $0k0$ ($k = 2n + 1$) and $h0l$, ($l = 2n + 1$), unambiguously indicated $P2_1/c$ as the space group. The structure was solved by direct methods. An analytical absorption correction, achieved by indexing the well-formed crystal faces [(001), (00$\bar{1}$), (1,1,0), ($\bar{1}$,$\bar{1}$,0), (1,$\bar{1}$,0), and ($\bar{1}$,1,0)] was applied to the data. Disorder from puckering of the five-membered Pd-dmpe ring was modeled by fixing site occupancy factors at 50% for all carbon atoms of the chelate C(2) to C(7) and C(2A) to C(7A). All other non-hydrogen atoms in the metal complex were refined anisotropically. The phenyl groups of the BPh_4 anion were all treated as isotropic rigid groups. All hydrogen atoms were generated in idealized positions for the structure factor calculations but were not refined.

A colorless cube-shaped crystal of **4** cut to the approximate dimensions 0.43 × 0.36 × 0.25 mm was used for the room-temperature crystal and intensity data collection. The unit cell parameters and systematic absences, $0kl$ ($k = 2n + 1$), $h0l$ ($l = 2n + 1$), $hk0$ ($h + k = 2n + 1$), $h00$ ($h = 2n + 1$), $0k0$ ($k = 2n + 1$), and $00l$ ($l = 2n + 1$), uniquely indicated $Pbcn$ as the space group. The structure was solved by direct methods. An absorption correction applied from ψ scan data did not significantly improve R, and therefore none was used. Disorder of the methylene carbons of the dmpe bound to Pd(2) was modeled by allowing the site occupancy factors for the two sets of the two methylene carbons (C(24), C(24A), C(25), C(25A)) to refine as free variables. The disordered BF_4

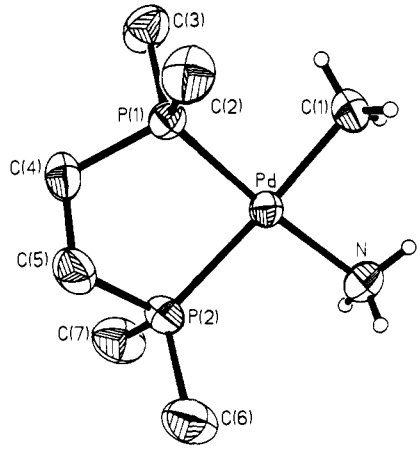

Figure 1. Thermal ellipsoid plot (50%) and atom numbering scheme for **1**.

Scheme I

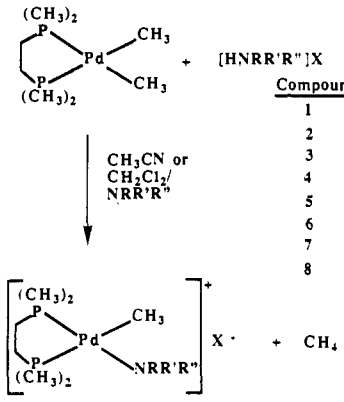

Compound	NRR′R″	X
1	NH_3	PF_6
2	NH_3	BPh_4
3	NH_2Et	BPh_4
4	$NHEt_2$	BF_4
5	$NHEt_2$	BPh_4
6	NEt_3	BPh_4
7	NH^iPr_2	BPh_4
8	1-methylimidazole	BPh_4

anions were treated as isotropic rigid groups with fixed bond lengths and angles. All non-hydrogen atoms, except for the disordered methylene carbons and the BF_4 groups, were allowed to refine anisotropically. All hydrogen atoms were generated in idealized positions for the structure factor calculations but were not refined.

An olive-colored cube-shaped crystal of **6** cut to the approximate dimensions 0.28 × 0.26 × 0.24 mm was used for the room-temperature crystal and intensity data collection. The unit cell parameters and systematic absences, $0k0$ ($k = 2n + 1$) and $h0l$ ($l = 2n + 1$), unambiguously indicated $P2_1/c$ as the space group. The structure was solved by direct methods. An absorption correction applied from ψ scan data did not significantly improve R, and therefore none was used. All non-hydrogen atoms were refined anisotropically except for boron and the phenyl groups, which were treated as isotropic rigid groups. All hydrogen atoms were generated in idealized positions for the structure factor calculations but were not refined. Atomic coordinates and isotropic thermal parameters for **1**, **3**, **4**, and **6** are contained in the supplementary material. Selected bond lengths and angles are given in Table II.

Results

Protonolysis of (Bis(dimethylphosphino)ethane)dimethylpalladium(II) by Ammonium Salts. The reaction between Pd(dmpe)Me_2 [dmpe = 1,2-bis(dimethylphosphino)ethane] and 1 equiv of ammonium salt [NHRR′R″]X in CH_3CN or CH_2Cl_2 yields methane and the cationic complex [Pd(dmpe)Me(NRR′R″)]$^+$, as shown in Scheme I. Similar reactions with phenol have also been observed.[13] At room temperature the protonolysis reactions are complete within seconds. The resulting solutions yield X-ray quality crystals of the cationic amine complexes after layering with ether for several days. With the exception of **6**, which gives olive crystals because of a small amount of decomposition during crystallization, all the compounds are colorless. In the solid state the amine complexes are air-stable for short periods of time. Prolonged exposure to moist air results in decomposition. Compounds **1–8** can be stored indefinitely under nitrogen at −20 °C.

Compounds **1–8** exhibit two distinct doublets in the $^{31}P\{^1H\}$ NMR spectrum (Table III) consistent with a square-planar palladium(II) geometry with two inequivalent cis phosphine moieties.[14] The upfield resonance, the phosphine trans to the coordinated amine (δ 14–21), was thus assigned because its chemical shift varies most as the amine varies. The ^{31}P resonance trans to the Pd–C bond lies between δ 37.1 and δ 38.5. The ^{31}P

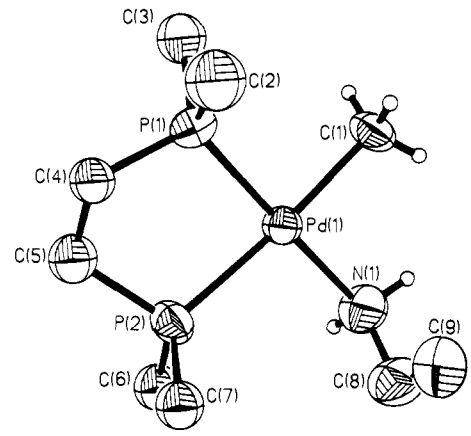

Figure 2. Thermal ellipsoid plot (50%) and atom numbering scheme for **3**.

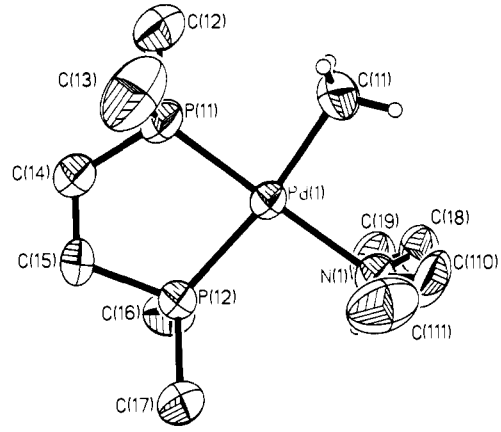

Figure 3. Thermal ellipsoid plot (50%) and atom numbering scheme for **4**.

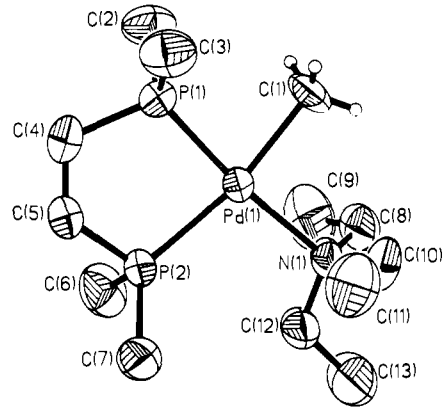

Figure 4. Thermal ellipsoid plot (50%) and atom numbering scheme for **6**.

(13) Kim, Y.-J.; Osakada, K.; Takenaka, A.; Yamamoto, A. *J. Am. Chem. Soc.* **1990**, *112*, 1096–1104.

(14) Pregosin, P. S.; Kunz, R. W. *^{31}P and ^{13}C NMR of Transition Metal Phosphine Complexes*; Volume 16, NMR Basic Principles and Progress; Drehl, P., Fluck, E., Kosfeld, R., Eds.; Springer-Verlag: Berlin, Germany, 1979.

Table II. Selected Bond Distances (Å) and Bond Angles (deg) for [Pd(dmpe)Me(NRR'R'')]X

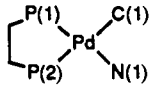

	1	3	4[a]	6
		Bond Distances		
Pd–P(1)	2.205 (2)	2.211 (2)	2.210 (3)	2.201 (3)
Pd–P(2)	2.336 (2)	2.316 (2)	2.331 (3)	2.366 (2)
Pd–C(1)	2.081 (4)	2.116 (7)	2.098 (11)	2.130 (8)
Pd–N(1)	2.139 (5)	2.147 (6)	2.182 (8)	2.244 (7)
		Bond Angles		
Pd(1)–Pd–P(2)	86.3 (1)	85.8 (1)	85.7 (1)	85.8 (1)
P(1)–Pd–C(1)	89.0 (2)	88.9 (2)	86.8 (3)	82.4 (3)
P(2)–Pd–N(1)	98.9 (1)	96.8 (2)	96.4 (2)	100.8 (2)
C(1)–Pd–N(1)	85.8 (2)	88.4 (3)	91.1 (4)	91.0 (3)

[a] Bond distances and angles are the average values for the two molecules in the unit cell. The numbering scheme for the table is different from Figure 3.

Table III. $^{31}P\{^1H\}$ NMR Data for [Pd(dmpe)Me(NRR'R'')]X[a]

compd	P{trans to N} (ppm)	P{trans to C} (ppm)	$^2J_{PP}$ (Hz)
1	21.44	38.50	22.0
2	20.18	38.14	21.5
3	18.31	37.56	19.5
4	17.00	37.10	18.4
5	19.06	38.50	18.7
6	14.83	37.06	17.6
7	13.80	37.31	17.5
8	20.81	37.84	21.1

[a] All spectra recorded in CD_2Cl_2 at room temperature.

resonances trans to the alkyl-substituted amines exhibit a progressive upfield shift as the number of alkyl substituents on nitrogen increases, but no correlation to basicity is observed.[15] The ^1H NMR spectrum displays a doublet of doublets splitting pattern for the metal bound methyl group consistent with the combination of cis and trans phosphorus coupling. The protons on the alkyl substituent bound to nitrogen exhibit a downfield shift upon coordination of the amine to the metal center. The remaining protons display normal resonances expected for each ligand system, as listed in the Experimental Section.

Molecular Structures of Amine Complexes. X-ray crystal structure determinations for **1**, **3**, **4**, and **6** (Figures 1–4) confirmed the cis square-planar geometry around palladium. Increasing the number of alkyl substituents on the coordinated amine results in a distortion from an ideal square-planar geometry about the metal. Bond angle distortions away from 90° only occurred in the plane of the molecule; there were no distortions out of plane. Increasing the number of amine alkyl substituents also had the effect of lengthening the palladium–nitrogen bond distance by 0.1 Å over the range of compounds studied. This phenomenon can be attributed to steric effects, as discussed later. Selected bond distances and angles are summarized in Table II.

Equilibrium Measurements of Amine Binding. By observing the $^{31}P\{^1H\}$ NMR resonances of the dmpe phosphorus trans to the amine group (Table III), the equilibrium constant of a free amine displacing coordinated amine could be measured. Addition of free amine to a CD_2Cl_2 solution of [Pd(dmpe)Me(NRR'R'')]X results in four distinct $^{31}P\{^1H\}$ resonances attributed to the pair of palladium amine complexes present in solution (Figure 5). Integration of these resonances allowed for the calculation of the relative equilibrium constants. Diethylamine was chosen as the standard (setting its $K = 1$) to quantify amine binding as shown in Table IV.

Changing the substituents on the nitrogen of the amine allowed for the examination of several trends. Replacing the hydrogens

(15) Grim, S. O.; Keiter, R. L. *Inorg. Chim. Acta* **1970**, *4*, 56–60.

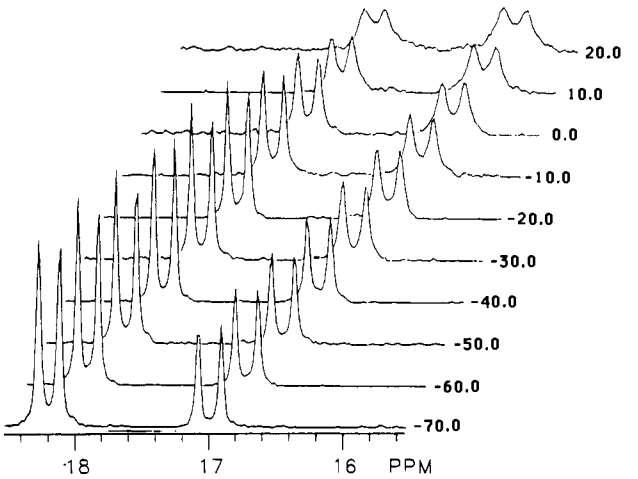

Figure 5. Variable-temperature $^{31}P\{^1H\}$ NMR data in °C for a sample equilibrium measurement for $NHEt_2$ and $NH_2{}^tBu$ binding to Pd(dmpe)Me$^+$. The upfield resonance is the dmpe phosphorus trans to the bound $NH_2{}^tBu$ and the other resonance is for the $NHEt_2$ complex. The solvent is CD_2Cl_2, which is 0.22 M in $NH_2{}^tBu$ and initially contained 0.036 M **5**.

Table IV. Equilibrium Formation Constants and pK_a Values for Amines Binding to [Pd(dmpe)Me]$^+$ and BMe_3

amine	K (20°, CD_2Cl_2)[a] [Pd(dmpe)Me]$^+$	K (100°, gas phase)[b] BMe_3	pK_a (CH_3CN)[c]
1-methylimidazole	20.0		–
ethylamine	2.2	14.2	18.40
2-methylaziridine	1.5		–
isopropylamine	1.0	2.72	17.92[d]
diethylamine	1.0	0.82	18.75
piperidine	1.0	47.6	18.92
ammonia	~0.9	0.22	16.46
pyridine	0.36	3.32	12.33
1-adamantanamine	0.29		18.14[e]
tert-butylamine	0.11	0.11	18.14
dicyclohexylamine	1.6×10^{-2}		17.88[f]
quinuclidine	8.7×10^{-3} [h]	51.0	18.46[g]
diisopropylamine	5.7×10^{-3}		17.88[f]
aniline	1.6×10^{-3}		10.56
trimethylamine	1.4×10^{-3} [h]	2.12	17.61
triethylamine	2.4×10^{-5}	<0.09	18.46

[a] Values calculated relative to diethylamine. [b] Taken from ref 11. [c] Taken from ref 21. [d] Estimated to be the same as isobutylamine. [e] Estimated to be the same as *tert*-butylamine. [f] Estimated to be the same as diisobutylamine. [g] Estimated to be the same as triethylamine. [h] Values measured in THF/C_6D_6 (see Experimental Section).

of ammonia with ethyl groups assigns the binding order as $NH_2Et > NHEt_2 > NH_3 \gg NEt_3$. Changing the substituent on a monosubstituted amine reveals a binding order $NH_2Et > NH_2{}^iPr > NH_2H >$ 1-adamantamine $> NH_2{}^tBu > NH_2Ph$. Another modification examined was the effect of enclosing the nitrogen in a ring system. This resulted in the following binding order 1-methylimidazole > 2-methylaziridine > $NHEt_2$ (no ring), piperidine > pyridine > quinuclidine. Ligand binding equilibrium constants were also measured over a range of temperatures for several different amines (Figure 5). Calculated values for ΔH from the van't Hoff equation gave rather small changes (on the order of the error of the measurements), so no reliable information could be extracted from this data. Because of broadening of the NMR resonances at higher temperatures (Figure 5), the variable-temperature data was essential for determining the reliability of the equilibrium constants (±10%).

Cone Angle Measurements for Amine Ligands. In order to quantify the contribution of steric effects to amine binding abilities, we measured amine cone angles. The cone angle concept, developed by Tolman for phosphine ligands,[1] has the advantage of placing amine ligands on a common steric scale with phosphines. For these measurements a wooden block containing a pin and

Table V. Measured Cone Angles for Amine Ligands (M–N = 2.2 Å)

amine	cone θ	amine	cone θ
NH_3	94	$NHCy_2$	133[a]
NH_2Me, NH_2Et, $NH_2{}^nPr$, $NH_2{}^iPr$, $NH_2{}^iBu$, NH_2Bz, NH_2 (neopentyl)	106	$NHPh_2$	136
		NH^iPr_2	137
NH_2Ph	111	NH^iBu_2	138
$NH_2{}^sBu$	113	$NHBz_2$, NMe_2Ph	140
NH_2Cy	115	$NMeEt^2$	145
$NHMe_2$, NHMeEt	119	NEt_3	150
piperidine	121	NH^sBu_2	158
$NH_2{}^tBu$	123	N^nPr_3	160
$NHEt_2$	125	NPh_3	166
NHMePh, NHEtPh	126	NEt_2Ph	170
NH_2(adamantyl), NH^nPr_2	127	NBz_3	210
NMe_3, quinuclidine, NMe_2Et	132	N^iPr_3	220

[a]This value was estimated from Figure 7, since the conformational degrees of freedom made it difficult to evaluate from molecular models.

plexiglass sidearm was cemented to a large protractor. A metal fitting to provide variable bond lengths (2.0–2.2 Å) was attached to the geometric center of the block and machined to accept CPK models. Cone angles measured for several phosphine ligands with this instrument were within 2° of those reported by Tolman.[3] A metal–nitrogen bond distance of 2.2 Å was used for the amine cone angles reported in Table V. This value was determined by taking an average of the palladium–nitrogen bond lengths observed in the crystal structure analyses described above. The effect of lengthening or shortening the assumed metal–nitrogen distance by 0.1 Å was to decrease or increase the cone angle by 4°.

As found for phosphine ligands there are problems in determining the minimum cone angle for complex ligands, because of the many internal degrees of freedom present.[16] Our estimates of minimum cone angles for strain-free ligand conformations cannot account for distortions of the other ligands bound to the metal center, which could also influence binding.

Discussion

Structural Evidence for Steric Strain. The palladium–nitrogen bonds in the cationic complexes studied show a range in bond distances of 0.10 Å. The shortest metal–nitrogen bond length is 2.139 (5) Å in **1**. This length exceeds the palladium–nitrogen distance reported for the cationic complex $[Pd(NH_3)_4]^{2+}$ at 2.004 (3) Å.[17] The increased bond length in **1** may be attributed to the trans influence of the phosphine as opposed to nitrogen,[18] as well as the greater electron density expected on Pd in **1**. The metal–phosphorus bond trans to the coordinated amine is an average of 0.12 Å shorter than that of the phosphorus trans to the methyl group in all four structures examined. A similar result has been reported for the compound Pt(dmpe)Me[NMe(Ph)],[19] which also exhibits a large trans influence for carbon.

The Pd–N distance of 2.244 (7) Å in **6** is the longest Pd–N bond reported to date,[20] and it even exceeds the trans Pd–P distance. We attribute this extremely long Pd–N bond distance to steric hindrance of the NEt_3 ligand. There appears to be little effect of basicity of the amine on the Pd–N bond length. The pK_a's of the free amines, measured in CH_3CN,[21] show no correlation with the Pd–N distances. A change of pK_a from 16.46 to 18.40 for NH_3 to NH_2Et, respectively, only accounts for a change in bond distance of 0.01 Å. Diethylamine, whose pK_a of 18.75 makes it the most basic of the series, has a bond length of 2.182 (8) Å, which is longer than either of the less basic NH_3 or NH_2Et. Triethylamine, whose pK_a resembles that of ethylamine (18.46), exhibits a metal–nitrogen bond 0.09 Å longer. Since the Pd–N distances show no correlation with amine basicity, we turned our attention toward steric parameters. The cone angles we measured for the amine ligands (Table V) closely parallel the Pd–N distances, as shown graphically in Figure 6. These steric parameters appear to have a major effect in determining the bond lengths for coordination of amines to the metal center.

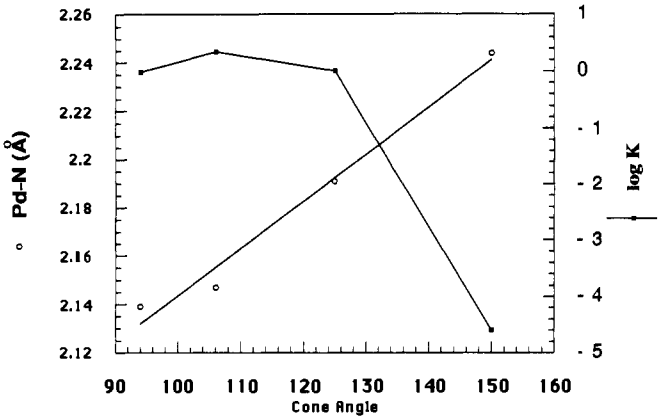

Figure 6. Plot of the Pd–N bond distances for **1**, **3**, **4**, and **6** (open circles) against the amine cone angles, which correlates linearly. Binding constants relative to **4** (solid squares) are also plotted against the amine cone angles, which show a poor correlation.

To gain a more thorough understanding of how steric hindrance of the amines effects the Pd–N bond lengths, it is helpful to examine the orientation of the alkyl substituents[16] of the coordinated amine. In the structures of **3** and **4** (Figures 2 and 3), it is apparent that the ethyl groups on nitrogen adopt a conformation limiting repulsive interactions with the remaining ligands bound to the metal center. For **4** the ethyl groups lie above and below the coordination plane of the complex. This limits their interaction with the methyl substituents on the phosphine and with the metal-bound alkyl. Interestingly, the β-hydrogen of the amines point away from the metal center.

The structure of **6** shows the orientation of two of the three ethyl groups of the coordinated triethylamine to be analogous to the diethylamine complex. The third ethyl substituent, however, must lie in the plane of the molecule. This greatly increases the steric interaction between the ethyl group and the methyl substituents on P(2). Here the β-hydrogens are directed toward the phosphine instead of the methyl of the ethyl group (Figure 4), which would be much more sterically demanding. This contrasts to the diethylamine complex whose out-of-plane ethyl groups direct back over the palladium thereby positioning their β-hydrogens away from the metal center. Brown proposed[11] for the structure of triethylamine that two of the three ethyl groups can orient themselves to the "back" of the nitrogen away from the lone pair. Because of steric hinderance, the third ethyl substituent must orient itself in the proximity of the lone pair, therefore limiting its accessibility.[22] This proposed structure differs from the orientation observed in the crystal structure of **6**, which shows that as many as two ethyl substituents on N can orient toward the front of the complexed nitrogen. Given the unknown importance of crystal packing in determining these configurations, we hesitate to speculate further about these observations.

The steric interactions discussed above not only result in the lengthening of the Pd–N bond distance but also distort the bond angles around palladium away from an ideal square-planar geometry. In strucutres **1**, **3**, **4**, and **6** the dmpe ligands form a puckered five-membered ring when coordinated to palladium.[20] In all four structures the P–Pd–P chelate bite angles are the same (86°) within experimental error (Table II). The remaining three

(16) (a) Alyea, E. C.; Dias, S. A.; Ferguson, G.; Restivo, R. C. *Inorg. Chem.* **1977**, *16*, 2329–2334. (b) DeSanto, J. T.; Mosbo, J. A.; Storhff, B. N.; Bock, P. L.; Bloss, R. E. *Inorg. Chem.* **1980**, *19*, 3086–3092.

(17) Christopher, F. J.; Michael, J. H. R. In *Comprehensive Coordination Chemistry: The Synthesis, Reactions, Properties and Applications of Coordination Compounds*; V, Late Transition Elements; Wilkinson, G., Ed.; Pergamon Press: 1987; Vol. 6, Chapter 51, p 1116.

(18) Huheey, J. E. *Inorganic Chemistry: Principles of Structure and Reactivity*, 3rd ed.; Harper and Row Publishers, Inc.: New York, NY, 1983.

(19) Bryndza, H. E.; Tam, W. *Chem. Rev.* **1988**, *88*, 1163–1188.

(20) Graaf, W.; Boersma, J.; Smeets, W. J. J.; Spek, A. L.; Koten, G. *Organometallics* **1989**, *8*, 2907–2917.

(21) Coetzee, J. F. *Prog. Phys. Org. Chem.* **1967**, *4*, 45–92.

(22) (a) Brown, H. C.; Sujishi, S. *J. Am. Chem. Soc.* **1948**, *70*, 2878–2881. (b) Brown, H. C.; Taylor, M. D. *J. Am. Chem. Soc.* **1947**, *68*, 1332–1336.

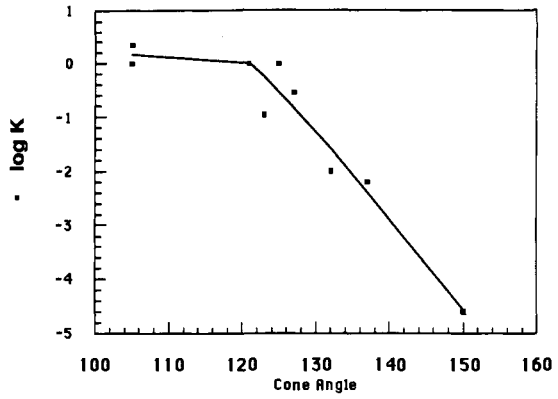

Figure 7. Plot of log K values vs cone angle (those amines which lie within a ±0.5 pK_a unit range) for the binding of NH_2Et, $NH_2{}^iPr$, $NHEt_2$, piperidine, $NH_2{}^tBu$, 1-adamantanamine, NH^iPr_2, quinuclidine, and NEt_3 to Pd(dmpe)Me^+.

angles in the square plane exhibit distortions that correlate with the steric bulk of the coordinated amines. These distortions only occur in the plane of the molecule. The most significant variations of bond angles are displayed in the structure of **6**. The N(1)–Pd–P(2) and N(1)–Pd–C(1) bond angles in **6** are maximized to provide more room for the bulky NEt_3 ligand. For the molecule to accommodate this change and maintain a planar geometry, there is a closing of the P(1)–Pd–C(1) bond of 4° in the triethylamine complex, as compared to the diethylamine complex. Only small changes in bond angles are observed when the structure of **3** is compared to that of **4**. This can be attributed to the ability of the ethyl substituents on the amines to orient themselves above and below the square plane of the molecule to relieve in-plane strain.

In the four structures it is evident that the N(1)–Pd–P(2) bond angle between cis substituents is more than 9° larger than the C(1)–Pd–P(1) bond angle. This occurs even in the case of **1**, where the NH_3 and CH_3 ligands are expected to have similar steric effects.[23] In **1** the Pd–N bond distance is 0.06 Å longer than the Pd–C bond in accord with the metal–carbon bond being stronger than the metal–nitrogen bond.[24] This may explain the bond angle dissimilarity, since the weaker Pd–N bond can be more easily deformed to reduce steric repulsions than the stronger Pd–C bond.

Equilibrium Binding Measurements and Steric Strain. The relative binding abilities for a wide range of amine ligands are provided in Table IV. In contrast to the excellent correlation between bond length and cone angles, the equilibrium binding constants correlate poorly with the ligand cone angles (Figure 6). Ammonia, which possesses the smallest cone angle, binds to the metal center less effectively than diethylamine, which has a cone angle 31° larger and a pK_a 2.29 units higher. In this series ethylamine is over twice as good a ligand as diethylamine, but triethylamine, whose pK_a is nearly the same as diethylamine with a cone angle 25° larger, is 4×10^4 weaker as a ligand (shown graphically in Figure 6). The series of monosubstituted amines NH_2Et, $NH_2{}^iPr$, NH_2H, 1-adamantanamine, $NH_2{}^tBu$, and $NHPh_2$ displays a similar pattern where both steric and electronic parameters contribute to their binding abilities. Ammonia and aniline have weaker binding abilities than expected for their cone angles of 94° and 111°, respectively, which makes them the two smallest ligands of the series. Binding constants for several amines with similar (±0.5 pK_a units) pK_a values are plotted against their cone angles in Figure 7. Steric effects should dominate binding affinities in this group, and a linear correlation is observed for amines with $\theta \geq \sim 120°$. Amines of smaller cone angle show little variation in their binding constant, which suggests the presence of a steric threshold.[4] Similar threshold behavior has been observed previously for the correlation of kinetic and thermodynamic data to the cone angle of phosphine ligands in transition-metal systems.[4a-e] For $\theta \leq \sim 120°$ only amine basicity should effect the equilibrium constants.

For all amine ligands above the steric threshold, neither steric nor electronic parameters alone can explain the binding affinities. The data can be fit to eq 1. The least-squares plane yields the

$$\log K = a + b(pK_a) + c(\theta) \quad (1)$$

values $a = 8.1$, $b = 0.54 \pm 0.04$, and $c = -0.15 \pm 0.01$ for amines above the steric threshold. This equation describes a plane, and the fit to the experimental points is shown in Figure 8. A pure steric contribution or a contribution solely from basicity effects would result in a plane sloped in only one direction. The calculated least-squares plane for the data presented displays a plane sloping in both directions north–south and east–west, which provides a graphical illustration of the importance of both effects. The error limits represent the maximum change in a coefficient necessary to put the worst-fitted data point on the least-squares plane. The residual or mean square error, σ, of the fitted log K values is 0.5. The multiple correlation coefficient, R, is 0.95. Since $R^2 = 0.91$, this implies that 91% of the variance is explained by regression of log K on the pK_a and θ values.[26]

The symbiotic relationship between steric and electronic effects is evident when examining the binding abilities of the three trisubstituted amines studied. Triethylamine, by far the weakest ligand studied, has a pK_a similar to that of diethylamine. Restricting the free rotation of the ethyl groups by effectively tying them back, as in quinuclidine, reduces the ligand cone angle and increases the binding ability 360-fold. This is apparently purely a steric phenomenon, since both amines should have similar pK_a values in solution.[27] Trimethylamine, which possesses the same cone angle as quinuclidine and has a pK_a ~0.8 units weaker,[27] is six times a poorer ligand.

Several cyclic amines were examined and exhibited a binding order of 1-methylimidazole > 2-methylaziridine > piperidine > pyridine > quinuclidine. This series contains both aromatic heterocycles and aliphatic amines. For 2-methylaziridine we observe a slight increase in binding strength above diethylamine that can be attributed to a decrease in the C–N–C angle. This must be a steric phenomenon, because the pK_a of 2-methylaziridine is less than that of diethylamine.[28] The cone angle of 2-methylaziridine was unmeasurable because of the limits of the CPK models, therefore it was estimated to be smaller than NHMeEt at 119°. This effect is not observed for piperidine, which exhibits the same equilibrium constant as diethylamine even though it has a smaller cone angle and a slightly greater basicity.

Pyridine and 1-methylimidazole, two different planar aromatic heterocycles, do not correlate well with equilibrium data for the other amines. These heterocyclic amines exhibit limited steric repulsion because of their planarity. They appear to bind to the metal center more effectively than expected from their pK_a values, even if one assumes they have no steric hindrance. Similar behavior was observed for Ru(II)–pyridine complexes,[25] and the increased binding ability of pyridines as compared to saturated amines was attributed to π back-bonding to the metal center. In a study of metal pentacarbonyl amine complexes, Dennenberg and Darensbourg observed a similar preference for pyridine ligands.[7] A plot of the negative log of the dissociation rate constant for the amine ligand versus its pK_a revealed two linear correlations; one for aliphatic amines and another for pyridines, which bound more effectively than expected. It is noteworthy that the two most

(23) In ref 3 Tolman reports the cone angle for CH_3 to be 90°.
(24) (a) Marks, T. J.; Schock, L. E. *J. Am. Chem. Soc.* **1988**, *110*, 7701–7715. (b) Bryndza, H. E.; Fong, L. K.; Paciello, R. A.; Tam, W.; Bercaw, J. E. *J. Am. Chem. Soc.* **1987**, *109*, 1444–1456.
(25) Shepherd, R. E.; Taube, H. *Inorg. Chem.* **1973**, *12*, 1392–1401.
(26) Afifi, A. A.; Azen, S. P. *Statistical Analysis*; 2nd ed.; Academic Press: New York, 1979; pp 144–171.
(27) Alder, R. W. *Chem. Rev.* **1989**, *89*, 1215–1223. The pK_a of quinuclidine in H_2O is reported herein as 10.95. Reference 21 reports the pK_a of triethylamine in H_2O as 10.65. We have assumed the pK_a of quinuclidine in CH_3CN to be the same as triethylamine; the pK_a difference may be even larger.
(28) The aqueous pK_a of aziridine in ref 27 is reported as 8.04. Reference 21 reports the pK_a of diethylamine in H_2O as 10.98. Decreases in C–N–C angles result in reduced basicities.

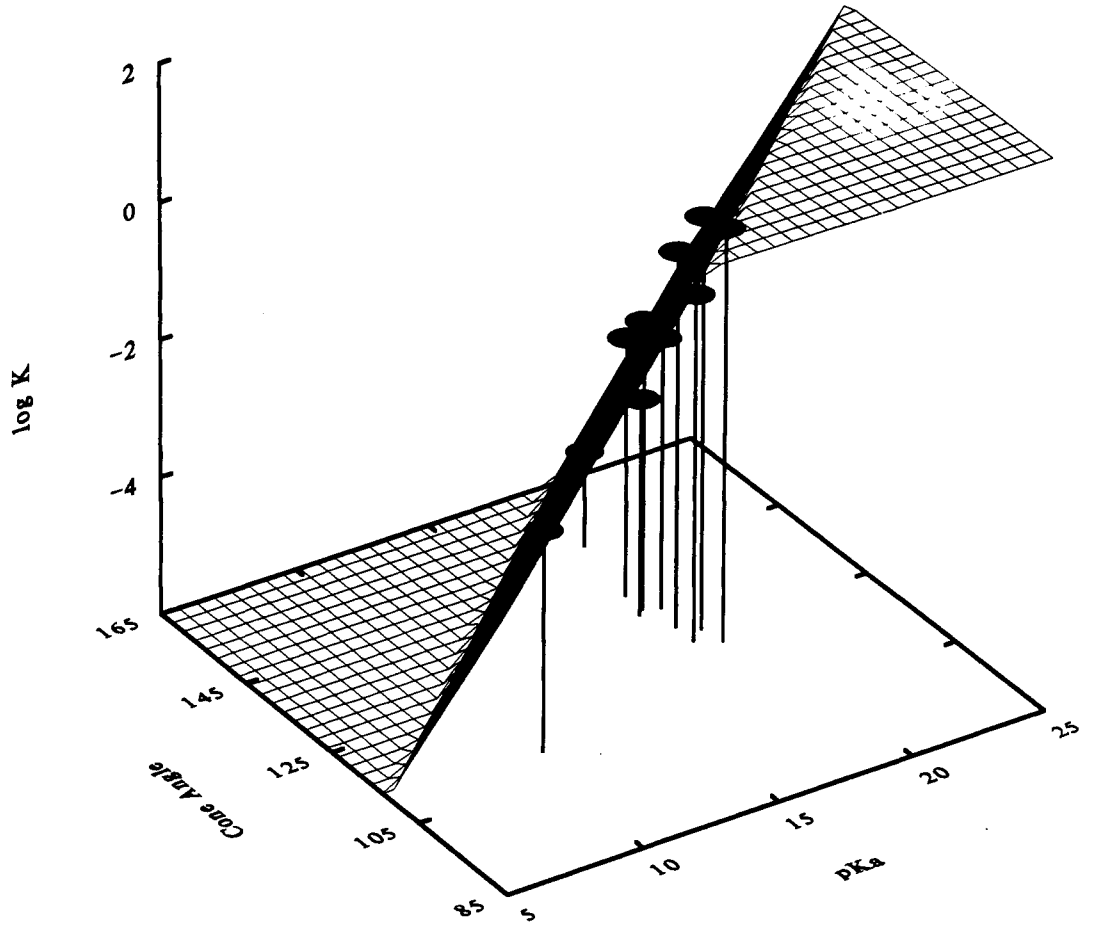

Figure 8. Log K values for the amines in Table V with $\theta \geq 120°$ plotted vs cone angle and pK_a. The surface represents the two-parameter least-squares fit to the data given by the equation $\log K = 8.1 + 0.54pK_a - 0.15\theta$.

effective amine ligands (1-methylimidazole and ethylamine) for Pd(II) in Table IV resemble those (i.e., histidine and lysine) residues often found to bind transition-metal ions in metalloproteins.

Conclusions

This study shows that amine ligand binding to transition metals can be quantitatively explained by using steric and electronic parameters similar to those used in studies of phosphine ligand binding. An important consequence is that this will allow comparisons of phosphines and amines on a common scale to quantitatively determine differences that might originate from hard–soft considerations. Such measurements are underway in our laboratories.

While the trends we have observed for amine ligand binding to Pd(II) seem to be the same as found for transition metals as diverse as Ru(II) and W(0), the correlation with main group systems is less impressive. Earlier studies of amine ligand binding to trimethylboron[11] show ammonia to be an anomalously weak ligand (Table IV), in contrast to data for transition metals. Quinuclidine and piperidine bind unusually well to trimethylboron. The boron Lewis acid data does not correlate well with amine pK_a's, gas-phase proton affinities,[29] cone angles, or combinations of these parameters. Since the B–N bonds are expected to be short, which will magnify steric effects and bond length distortions, this may account for some of the variation. However, one feature common to the transition metal and boron Lewis acid systems is the anomalous high binding affinity of pyridine. In the boron system one would have to use hyperconjugative interaction between a π-system combination of the three B–C σ bonds and a suitable empty π^* orbital of pyridine if one were to invoke π-bonding arguments. Theoretical studies might help answer these questions.

Acknowledgment. This work was supported by the National Science Foundation (Grant CHE-88-15958).

Supplementary Material Available: Tables of bond lengths, bond angles, anisotropic displacement coefficients, H-atom coordinates, and atomic coordinates with isotropic thermal parameters (14 pages); tables of observed and calculated structure factors (86 pages). Ordering information is given on any current masthead page.

(29) Aue, D. H.; Browers, M. T. In *Gas Phase Ion Chemistry*; Bowers, M. T.; Ed.; Academic Press: New York, 1979; Vol. 2, Chapter 9.